PID Control with Feedforward Using the Temperature Control Lab Kit

Thierry Tchanteu Moumi and Basil Mannaerts

Academic Year 2023-2024

Abstract

This report presents the application of control theory, particularly PID control with feedforward, using the Temperature Control Lab (TCLab) kit. It encompasses the design choices, experimental setup, and results, aiming to transfer the acquired knowledge to colleagues with a foundational understanding of control theory. The report refrains from theoretical reminders but focuses on practical implementation and analysis.

Contents

1 Introduction

In the pursuit of understanding and applying control theory to practical systems, the Temperature Control Lab (TCLab) kit serves as an excellent platform. This lab focuses on the implementation of a PID control strategy with feedforward control to manage the temperature within the TCLab environment effectively. The control system diagram provided (Figure 1) illustrates the structure of the control system that we aim to implement.

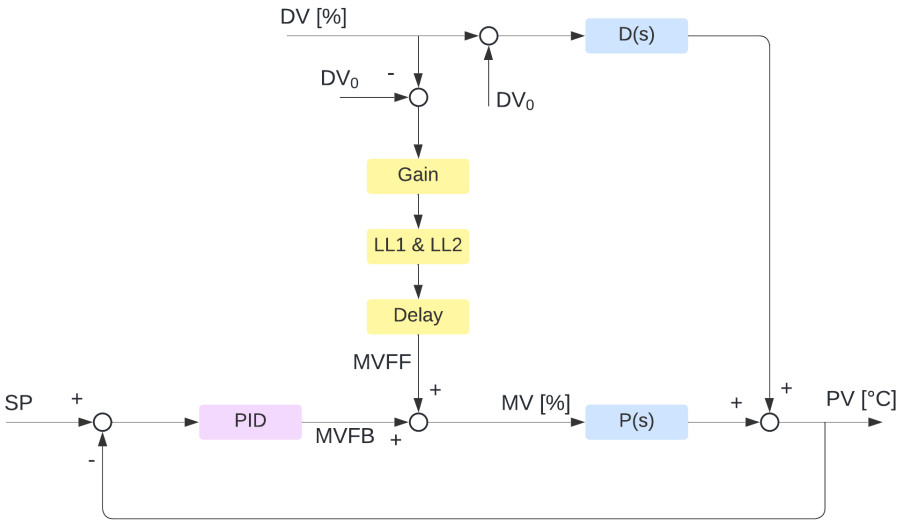

Figure 1: Control system diagram depicting the PID control with feedforward architecture. The system includes setpoint (SP), manipulated variable (MV), disturbance variable (DV), process variable (PV), and their interactions through the control elements like PID controller, gain, lead-lag compensators (LL1 & LL2), and delay elements.

The PID controller is designed to respond to the setpoint (SP), while the feedforward elements react to changes in the disturbance variable (DV). These components work together to regulate the manipulated variable (MV) which controls the heating power to the TCLab. This power adjustment affects the process variable (PV), the temperature, which we aim to control.

1.1 Lab Specifications

- **Platform:** Temperature Control Lab (TCLab) kit.
- **Control Objective:** To maintain the temperature at a setpoint value despite external disturbances.
- **Variables:**
  - Setpoint (SP): Desired temperature.
  - Manipulated Variable (MV): Heating power of heater 1 (%).

  - Disturbance Variable (DV): Heating power of heater 2 (%), acting as an external disturbance.
  - Process Variable (PV): Temperature of sensor 1 (°C).

- **Control Components:**
  - PID Controller: Adjusts the MV based on the difference between SP and PV.
  - Feedforward Control (MVFF): Compensates for the measured disturbance DV.
  - Lead-Lag Compensators (LL1 & LL2): Provide phase lead or lag to improve the system's response.
  - Delay: Models the inherent time delay in the system.

- **Software and Tools:**
  - Anaconda Distribution with Python for running simulation and control scripts.
  - Tkinter package for creating graphical user interface elements.
  - Custom Python package ('package LAB.py') for implementing the lead-lag function and the PID controller.
  - JupyterLab environment for executing and documenting the code.

- **Experiments Conducted:** A series of open-loop and closed-loop experiments to identify process dynamics and validate the control strategies.

The following sections will delve into the detailed procedures, results, and analyses of the control system's performance under various conditions as per the lab assignment's requirements.

2 Experimental Setup and Operation

The experimental setup comprises both hardware components, primarily the Temperature Control Lab (TCLab) kit, and software components for control and data acquisition. The following section delineates the procedure and methodology employed in utilizing the TCLab kit in conjunction with the associated software.

2.1 Hardware Configuration

- The TCLab kit is the centerpiece of the hardware setup, consisting of heating elements and temperature sensors. The heaters serve as the actuators in our control experiments, while the temperature sensors provide feedback to the control algorithms.

- The Arduino microcontroller integrated within the TCLab is employed for interfacing between the hardware components and the software layer.

2.2 Software Workflow

- The TCLab is controlled via a Python interface that communicates with the kit's microcontroller. This interface facilitates the implementation of control algorithms, manipulation of the heaters, and real-time data acquisition from the temperature sensors.
- Analysis of the acquired data is conducted using Python libraries. The `NumPy` library is utilized for numerical computations, `pandas` for data management, and `matplotlib` for plotting and visualizing the data.
- The `package_DBR` library, specifically designed for this course, includes custom functions for executing model identification routines, parameter estimation, and optimization algorithms required for controller tuning.

2.3 Operational Procedure

- The experiment is initiated by preheating the TCLab to a stable operating temperature to ensure a consistent starting point for all tests.
- A series of step changes are applied to the heater levels (manipulated variables) via the Python interface. The TCLab's response, primarily the temperature change (process variable), is logged for each step change.
- Data from the experiments are processed to analyze the step response of the system, which informs the subsequent model identification and controller design stages.

3 Open-Loop Control Experiments on Manipulated and Disturbance Variables

We conducted two sets of open-loop control experiments using the TCLab kit to examine the system's response to steps in manipulated variable (MV) and disturbance variable (DV).

3.1 Experiment on Manipulated Variable (MV)

In the MV step experiment, we observed the system's response to a sudden increase in the manipulated variable (MV). Initially, the MV was held constant at 30% of its maximum value. At $t = 0s$, the MV was abruptly increased to 70% and maintained at this new level for the duration of the experiment (MVo- delta to MVo+ delta. The delta value for our experience is 20%. A delta that is too small can be drowned out by noise). The resulting change in the process variable (PV) is shown in Figure 2. The PV rose noticeably in response to the MV step change, demonstrating the process dynamics and the system's ability to affect the PV based on the MV input.

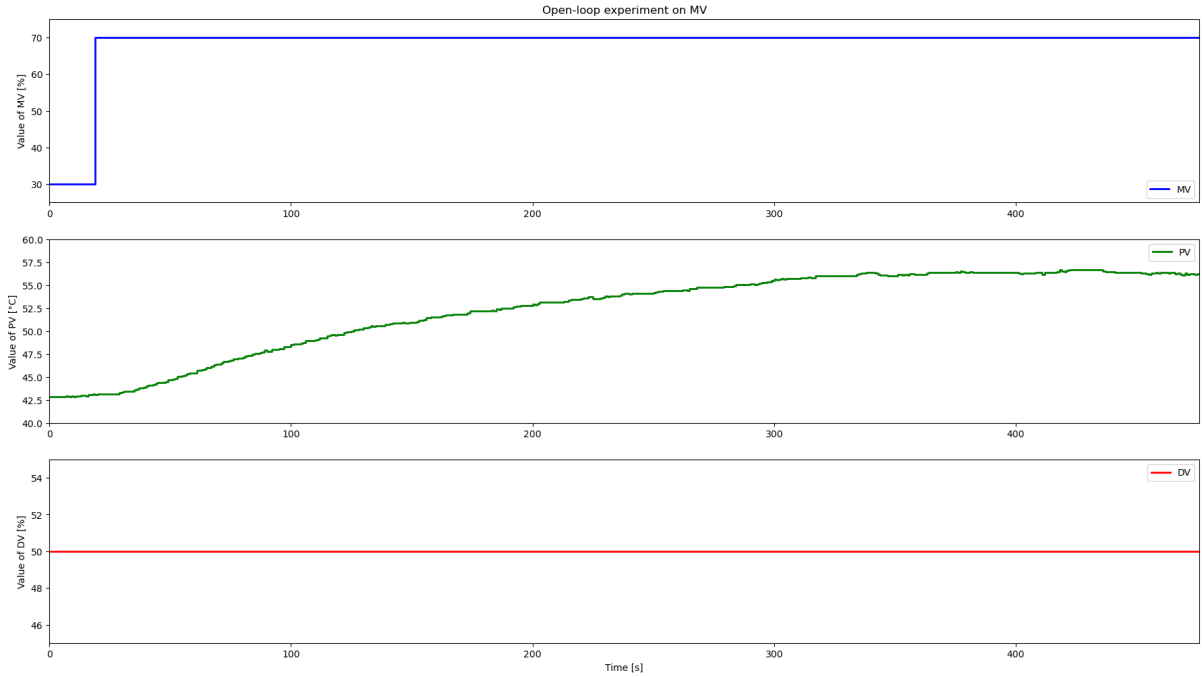

Figure 2: Open-loop experiment demonstrating the impact of a step change in the manipulated variable (MV) on the process variable (PV).

3.2 Experiment on Disturbance Variable (DV)

Following the MV experiment, we conducted a step experiment on the disturbance variable (DV). The MV was held constant, and at $t = 0s$, the DV was increased from 30% to 70% of its value. The PV's response, depicted in Figure 3, shows a gradual rise, highlighting the system's vulnerability to external disturbances. This increase in PV demonstrates the need for a control strategy capable of countering such disturbances.

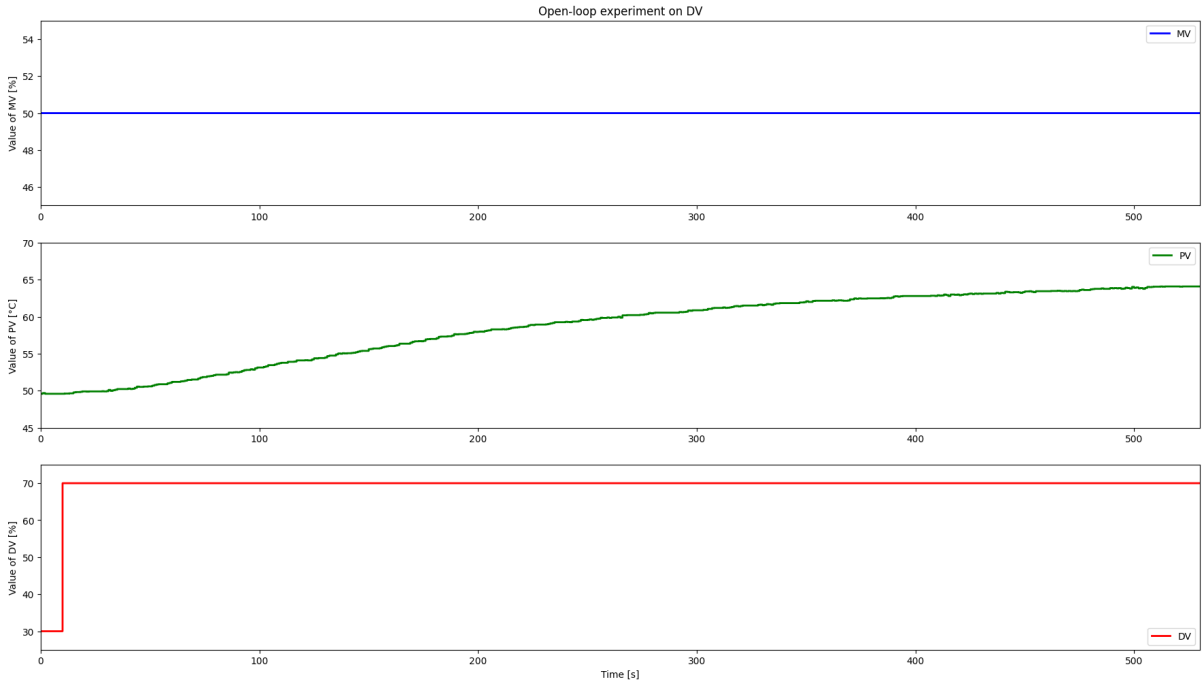

Figure 3: Open-loop experiment showing the effect of a step increase in the disturbance variable (DV) on the process variable (PV).

3.3 Discussion

The insights gained from these open-loop experiments are instrumental in comprehending the behavior of the TCLab kit. The MV experiment showcases the direct impact of control actions on the system's output, while the DV experiment emphasizes the system's sensitivity to external disruptions. Both experiments are vital for developing an understanding of the different influences on the PV and for formulating effective control strategies. Specifically, the MV step response is crucial for identifying the system's open-loop transfer function, which is a key component in the tuning of controllers. Conversely, the response to the DV step provides a clear picture of how disturbances affect the system, information that is fundamental for creating disturbance observers or implementing feedforward control mechanisms.

4 Model Identification of TCLab Dynamics

Model identification is a critical step in control system design. It involves developing a mathematical model that accurately represents the system's response to changes in inputs. For the TCLab kit, we focus on identifying a Second Order Plus Dead Time (SOPDT) model that characterizes the system dynamics in response to both Manipulated Variable (MV) and Disturbance Variable (DV).

4.1 Optimization Methodology

The identification process employs an optimization technique to minimize the sum of squared errors (SSE) between the experimental process variable (PV) and the estimated PV from the model. The model parameters, such as gain (K), time constants (T1, T2), and delay (theta), are adjusted iteratively using Powell's method, a derivative-free optimization algorithm. The aim is to find the parameter set that best fits the experimental data.

4.2 Identification Results

The identification experiments were conducted by implementing step changes in MV and DV and recording the PV's response. The plots of the experimental PV against the estimated PV, shown side by side for both DV and MV cases, visually represent the accuracy of the SOPDT models obtained.

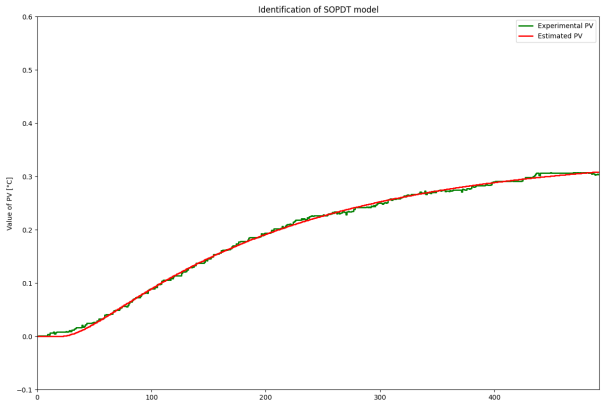

Figure 4: figure
Identification of SOPDT model for DV to PV.

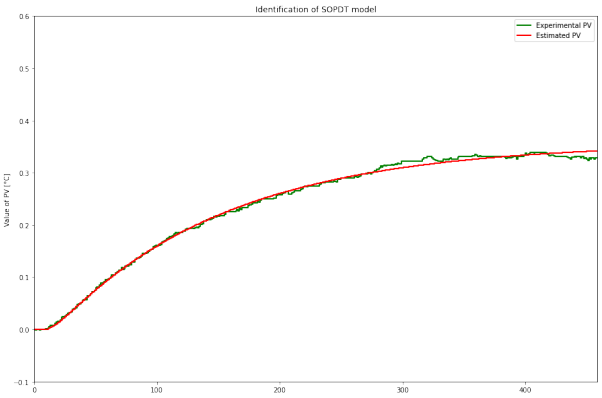

Figure 5: figure
Identification of SOPDT model for MV to PV.

For the DV to PV identification, the final SSE objective was 0.0066, indicating a close match between the model and experimental data. The estimated parameters were:

- Gain, K_d: 0.3412
- First time constant, $T1_d$: 190.0 seconds
- Second time constant, $T2_d$: 21.76 seconds
- Dead time, θ_d: 18.22 seconds

Similarly, the MV to PV identification yielded an SSE objective of 0.0130. The model parameters for this case were:

- Gain, K_p: 0.3571

- First time constant, $T1_p$: 140.0 seconds
- Second time constant, $T2_p$: 7.92 seconds
- Dead time, θ_p: 7.36 seconds

These parameters encapsulate the intrinsic dynamics of the TCLab's thermal system, providing a foundation for designing PID controllers or other control strategies.

4.3 Discussion

The identified SOPDT models accurately predict the TCLab's response, as evidenced by the minimal SSE objectives. The identification process underscores the slower dynamics and larger delay in response to DV changes compared to MV changes, which is typical for disturbance variables. This detailed understanding of the system's dynamics is crucial for implementing effective control strategies that can compensate for these delays and ensure precise temperature regulation within the TCLab system.

5 Comprehensive Model Identification

This section details the model identification process for the MV to PV system. The process involves both optimization-based methods and classical graphical approximations, culminating with a comparison of frequency response via Bode plots for each identified model.

5.1 Optimization-Based Identification

An SOPDT model was fitted to the experimental data through numerical optimization, which aimed to minimize the SSE between the actual PV and the model's estimated PV.

5.1.1 Optimization Outcomes

The optimized parameters for the MV to PV model were found to be: $K_p = 0.3571$, $T_{1p} = 140.004\,s$, $T_{2p} = 7.923\,s$, $\theta_p = 7.356\,s$ with an SSE of 0.0130. For DV to PV, the parameters were $K_d = 0.3412$, $T_{1d} = 189.997\,s$, $T_{2d} = 21.759\,s$, $\theta_d = 18.217\,s$, achieving an SSE of 0.0066.

5.2 Graphical Identification Using Manual Data

The graphical identification process involved manual data extraction from the step response curve, providing estimates for the model parameters using the Broida, van der Grinten, and Strejc methods.

5.2.1 Graphical Method Measurements

The step response curve was manually analyzed to extract K_p, a, T_u, T_g, t_1, and t_2.

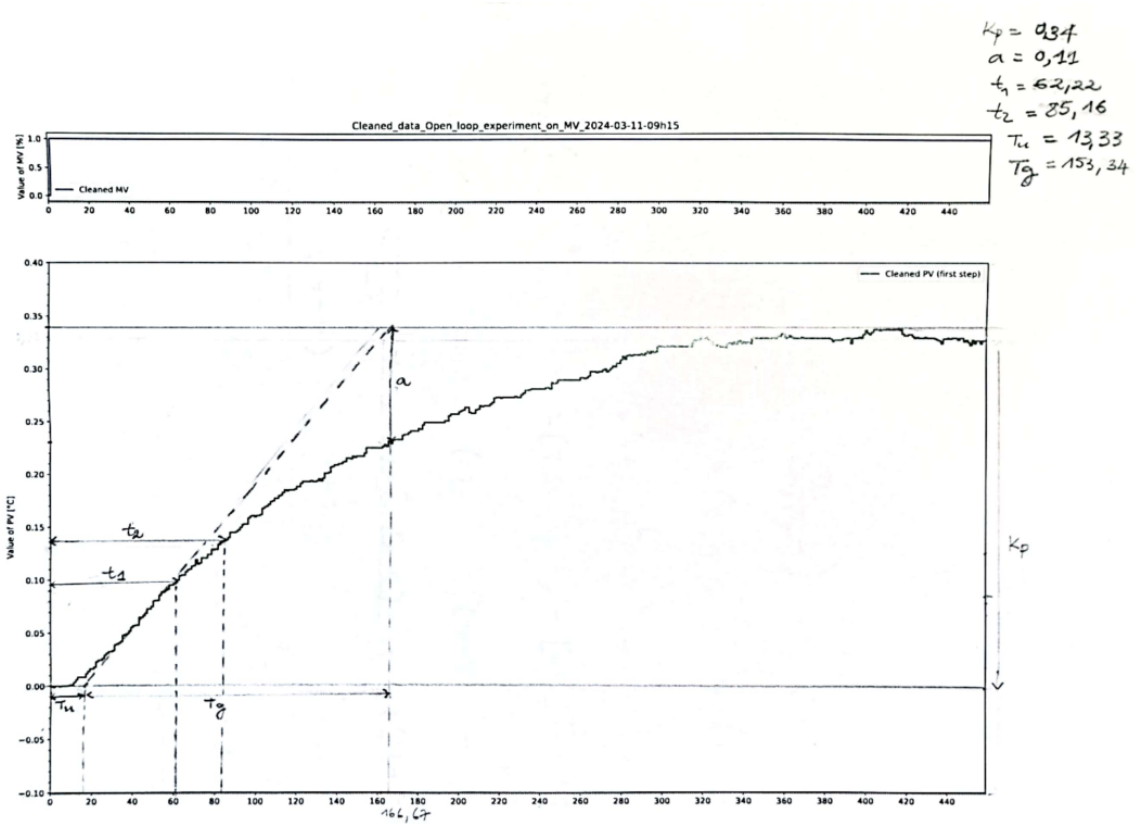

Figure 6: Manual data extraction from the experimental step response for model identification.

5.3 Broida Model (FOPDT)

The Broida method yields a First Order Plus Dead-Time (FOPDT) model, defined by the transfer function:

$$P_B(s) = \frac{K_p e^{-\theta s}}{Ts + 1}$$

Two distinct models were derived:

- **Model 1:** Utilizing a direct method, where T is equated to T_g and θ to T_u, giving us $T = T_g$ and $\theta = T_u$.
- **Model 2:** By graphical analysis using the tangent at the inflection point, we computed the time constant T and dead time θ as $T = 5.5(t_2 - t_1)$ and $\theta = 2.8t_1 - 1.8t_2$, respectively.

5.4 Van der Grinten Model (SOPDT)

The Van der Grinten method provides a Second Order Plus Dead-Time (SOPDT) model with the transfer function:

$$P_{vdG}(s) = \frac{K_p}{(T_1 s + 1)(T_2 s + 1)} e^{-\theta s}$$

The parameters T_1 , T_2 and θ were derived based on the system's response characteristic a. The equations:

$$T_1 = \frac{T_g(3ae - 1)}{1 + ae} \quad \text{and} \quad T_2 = \frac{T_g(1 - ae)}{1 + ae}$$

$$\theta = T_u - \frac{T_1 T_2}{T_1 + 3T_2}$$

However, the application of this method faced challenges, as the computation led to a negative T_1, which lacks physical meaning. Consequently, this SOPDT model was deemed invalid for our system. We can therefore conclude that system is unstable.

5.5 Strejc Model

The Strejc method, ideal for approximating higher-order systems with identical time constants, was also considered but resulted in a simplistic first-order model akin to the Broida model. The corresponding order n for the system was determined to be one, given the ratio $\frac{T_u}{T_g}$ fell between the Strejc parameters a_n for orders zero and one.

5.6 Comparative Model Analysis

The identified models, including the SOPDT from optimization and the Broida and Strejc models from manual data, were compared against the experimental data. The objective was to assess the accuracy of different modeling approaches.

5.6.1 Visual Comparison

The models' estimated PV responses were plotted alongside the cleaned experimental data for visual evaluation.

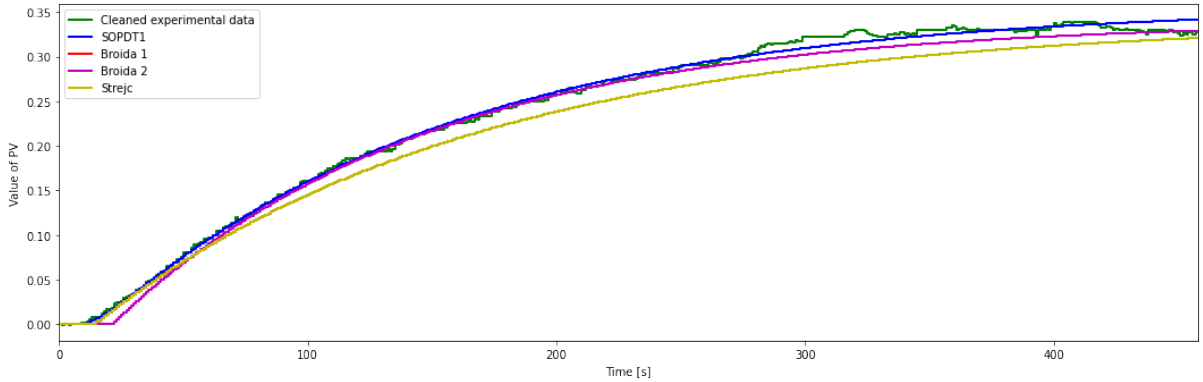

Figure 7: Overlay of experimental PV data with responses from different identified models.

5.7 Frequency Response Analysis

Finally, the frequency response of each model was analyzed using Bode plots. This analysis allows for the evaluation of how well each model captures the dynamics of the system across a range of frequencies.

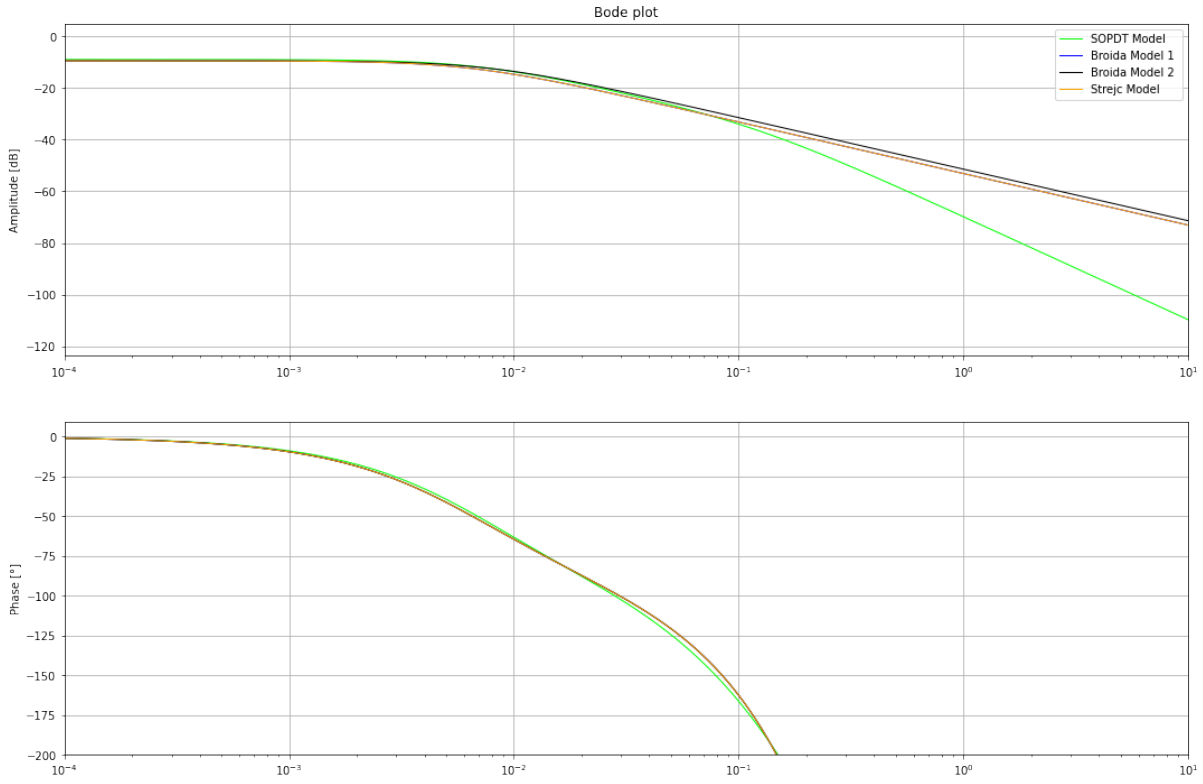

Figure 8: Bode plots for the SOPDT, Broida, and Strejc models based on the MV to PV identification.

5.8 Discussion

The optimization-based SOPDT model showed a high fidelity in capturing the system's dynamics, as evidenced by the SSE values. Graphical methods provided a reasonable first approximation but encountered challenges in certain scenarios, such as with the van der Grinten model. The Bode plots demonstrate how these models behave in the frequency domain, with the optimization-based model typically showing a better fit to the actual system.

6 Lead Lag and PID Implementation

The control strategy employed in the Temperature Control Lab (TCLab) combines the precision of Proportional-Integral-Derivative (PID) control with the preemptive action of feedforward control. Central to this approach is the implementation of lead-lag compensators and the PID controller, which are designed to manage the system's response to setpoint changes and disturbance variables effectively.

6.1 Lead Lag Compensator

The lead-lag compensator is used to improve the phase margin and stabilize the response. It achieves this by introducing a phase lead (speeding up the response) through T_{lead} and a phase lag (slowing down the response) through T_{lag}, thereby shaping the frequency response of the system to desired specifications. In the TCLab, the lead-lag compensator parameters directly influence the system's transient and steady-state behavior. A decrease in T_{lead} relative to T_{lag} generally results in a faster response to changes in the manipulated variable (MV), but can also induce more overshoot. Conversely, a larger T_{lag} can stabilize the system further but at the expense of responsiveness.

We implemented multiple methods of discretization, such as the Euler backwards difference, the Euler forward difference and the trapezoidal method, which mathematical developments can be seen in the Appendices of this report.

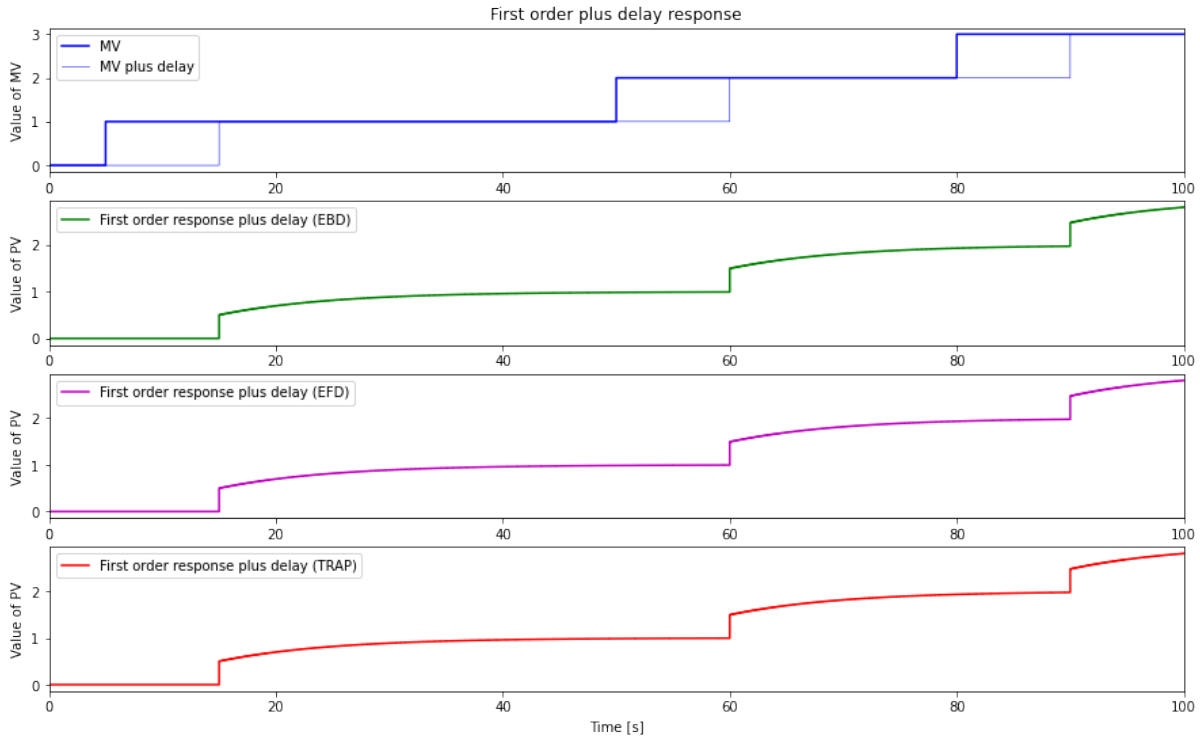

Figure 9: The response of the system with different lead-lag compensator settings. The blue line represents the manipulated variable (MV), and the other lines show the system output (PV) with various lead and lag times.

6.2 PID Controller

The PID controller is employed to dynamically adjust the system to maintain the process variable (PV) at the setpoint (SP). The controller's parameters, K_c, T_i, and T_d, are pivotal:

6.2.1 Mathematical Representation of PID Controller

The PID controller's action is encapsulated in its transfer function, which is represented as follows:

$$MV_{PID} = K_c \left(1 + \frac{1}{T_{I,s} \cdot s} + \frac{T_{D,s} \cdot s}{\alpha \cdot T_{D,s} \cdot s + 1}\right) \cdot E \tag{1}$$

In Equation 1, K_c is the proportional gain, $T_{I,s}$ the integral time constant, $T_{D,s}$ the derivative time constant, α a filter coefficient to attenuate the derivative action's noise sensitivity, and E the control error, which is the difference between the setpoint and the process variable.

- K_c (proportional gain) influences the magnitude of the controller's response to the error signal. A higher K_c increases the system's sensitivity to errors, leading to a faster but potentially less stable response.

- T_I (integral time) determines how quickly the controller accumulates the past error to eliminate steady-state offset. A smaller T_I will lead to a faster error correction but can cause instability if too small.

- T_D (derivative time) predicts future errors, allowing the controller to take preemptive actions. A larger T_D can smooth the response, but excessive T_D may lead to noise amplification.

The interaction between these parameters must be carefully balanced to achieve a stable and responsive control system.

Figures 9 and 10 illustrate the effects of the lead-lag compensator and the PID controller on the TCLab's response. The graphs depict the MV's step response with varying lead-lag parameters and the PID control action over time, including the proportional (P), integral (I), and derivative (D) contributions.

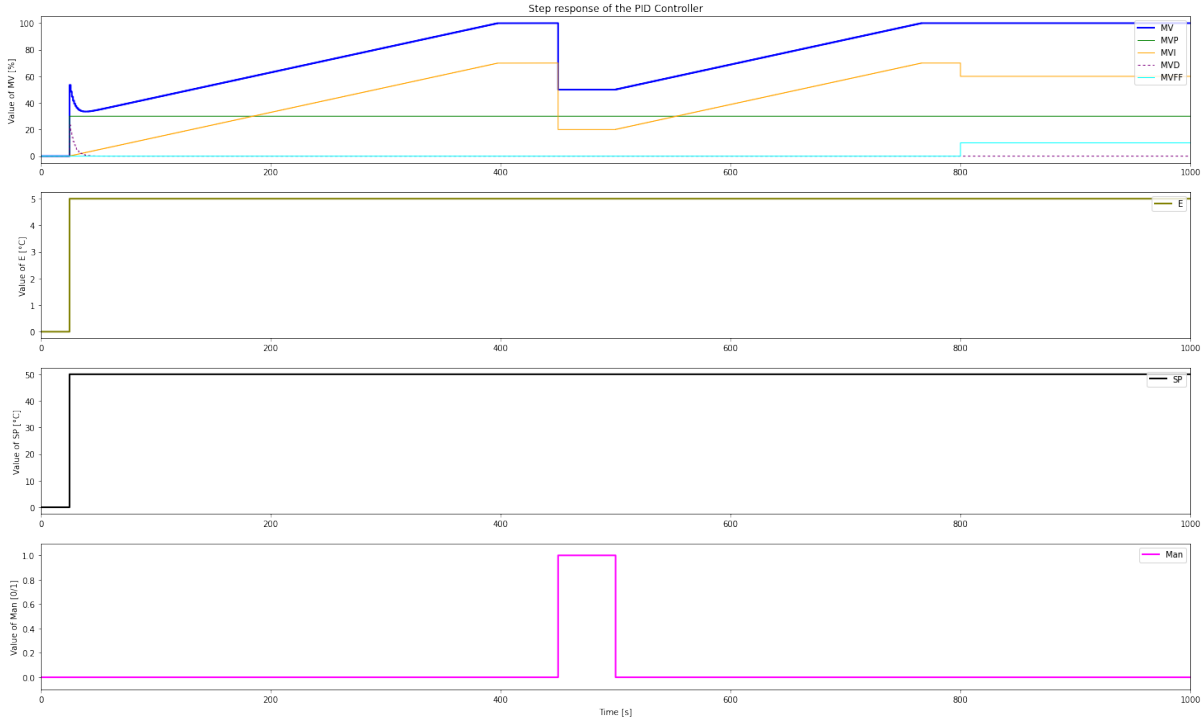

Figure 10: The PID controller response showing the separate contributions of the proportional (P), integral (I), and derivative (D) actions over time. Each subplot highlights the effects of adjustments in the PID parameters on the control signal (MV).

In summary, the lead-lag compensator and PID controller parameters were adjusted to optimize the system's performance, taking into consideration the trade-offs between speed and stability. This delicate balance ensures that the TCLab operates efficiently under varying conditions and disturbances.

7 IMC Tuning

In the context of the TCLab, IMC tuning was employed to determine the optimal PID controller parameters that would yield a desirable balance between system responsiveness and stability. This tuning method uses a model of the process to predict the future outputs and adjusts the control parameters accordingly.

The IMC tuning is based on the process dynamics characterized by the system's gain (K_p), primary and secondary time constants ($T1_p$ and $T2_p$), and the delay time (θ_p). For disturbance dynamics, similar parameters (K_d, $T1_d$, $T2_d$, and θ_d) are utilized. The objective is to match the controller's action with the inverse dynamics of the process, thus reducing the error between the setpoint and the process variable.

Given the following process parameters obtained from the identification phase:

- Process Gain, K_p: 0.357
- Primary Time Constant, $T1_p$: 140.0 s
- Secondary Time Constant, $T2_p$: 7.92 s
- Process Delay, θ_p: 7.36 s

and the disturbance dynamics parameters:

- Disturbance Gain, K_d: 0.341
- Primary Time Constant, $T1_d$: 190.0 s
- Secondary Time Constant, $T2_d$: 21.76 s
- Disturbance Delay, θ_d: 18.22 s

Given that we are in the presence of second order systems, we can use the formula case I from the table viewed in the control theory course, taking care to set T_3 to zero. The IMC tuning yielded the following PID parameters:

- Proportional Gain, K_c: 2.81
- Integral Time, T_i: 147.93 s
- Derivative Time, T_d: 7.50 s

The gamma parameter, which adjusts the aggressiveness of the control action, was set to 1 to ensure a balanced response. These parameters dictate how the PID controller responds to the error between the setpoint and the process variable. A smaller K_c value ensures a more stable system with less overshoot, while the integral and derivative times were set to minimize the steady-state error and anticipate future errors, respectively.

This model-based approach to PID tuning provides a systematic and reliable method to achieve good control performance. It allows for anticipatory adjustments to the controller settings, ensuring that the system reacts appropriately to both the setpoint and disturbances.

8 Stability Margins : Gain and Phase Margins

Gain and phase margins are key indicators of stability and performance for a PID controller. They assess the the robustness of the control system in terms of gain and phase delay.

- Gain Margin : that is the amount by which the system gain can be increased before the system becomes unstable.
- Phase Margin : that is the amount by which the system phase can be delayed before the system becomes unstable.

To determine these margins in the context of our laboratory, we started by determining the transfer function L(s) = P(s) x C(s). By applying the method for calculating these margins, we were able to determine a gain margin of 18.96 dB and a phase margin of 87.21°, as illustrated in the figure 11.

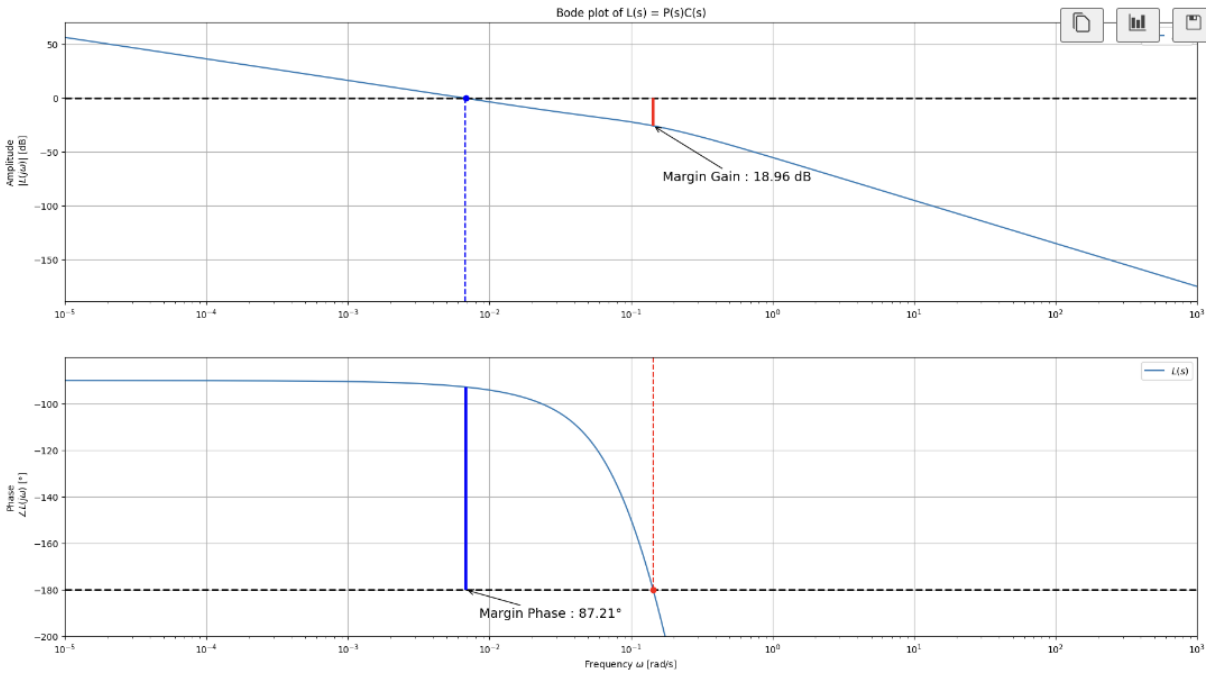

Figure 11: Graph of Gain and phase Margins.

A positive gain margin and positive phase margin indicate good stability and sufficient robustness margins of the system. However, excessively high margins can lead to slow system response. Conversely, low or negative margins indicate a system close to instability and may result in undesirable oscillations or unstable behavior. Our results are not far off from the ranges defined in the course for phase and gain margins. We can conclude that our system has a good margin of robustness.

9 Comparative Simulation Analysis

In this section, we analyze four distinct scenarios: two in an open-loop configuration (OLP) and two in a closed-loop (CLP), each with and without the implementation of feedforward (FF) control. These scenarios are meant for us to have a understanding of the system's reaction to changes in manipulated variables (MV), disturbance variables (DV), and the implementation of manual control (Man) as well as feedforward action (FF).

9.1 Open-Loop Response without Feedforward (OLP No FF)

In the first scenario, the system operates in an open-loop configuration without feedforward control, as shown in Figure 12. Here, the MV follows a predetermined path, unaffected by changes in the process variable (PV). The system's inability to react to an increase in disturbance (DV) is evident as there is no compensatory action taken to counteract its effects, leading to a disparity between the setpoint (SP) and the PV.

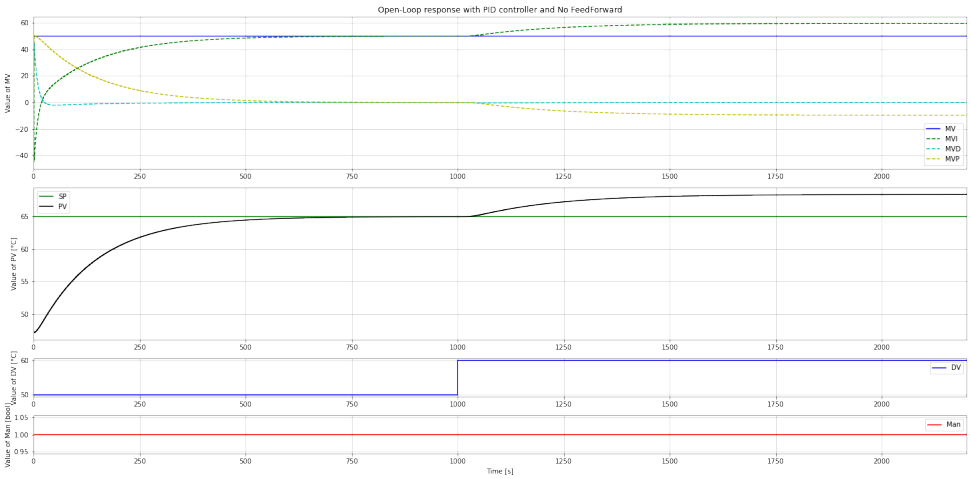

Figure 12: System response in an open-loop with no feedforward, showing the PV deviating from the SP in response to the disturbance.

9.2 Open-Loop Response with Feedforward (OLP FF)

The second scenario implements feedforward control while still in an open-loop configuration, illustrated in Figure 13. The MV is now influenced by the feedforward action which anticipates changes in DV. This proactive adjustment minimizes the impact of disturbances on the PV, maintaining it closer to the SP. The effectiveness of feedforward control in open-loop is thus underscored.

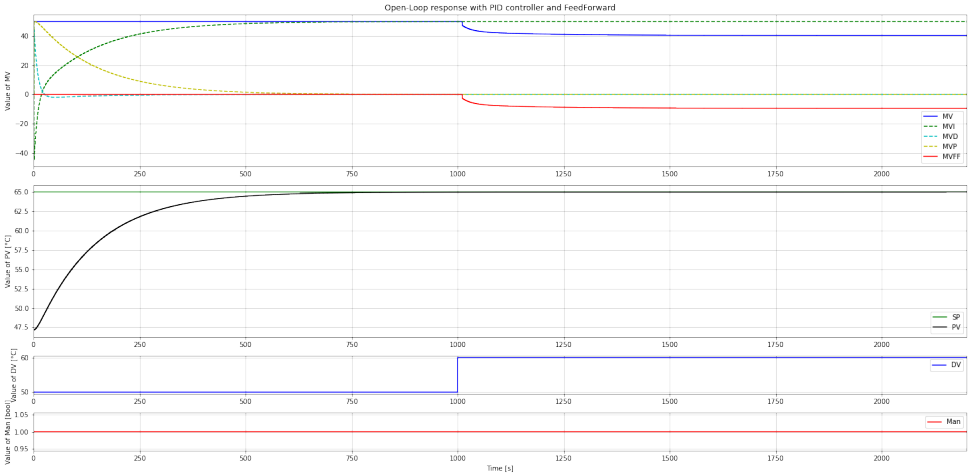

Figure 13: Open-loop system response with feedforward action showing improved PV tracking of the SP despite disturbances.

9.3 Closed-Loop Response without Feedforward (CLP No FF)

In the third scenario, the system transitions to a closed-loop operation without feedforward, as depicted in Figure 14. The introduction of the closed-loop allows the PID controller to dynamically adjust MV in response to the difference between SP and PV. Despite the absence of FF, the system exhibits a self-correcting behavior, reducing the PV deviation from the SP post disturbance, albeit with a slower response.

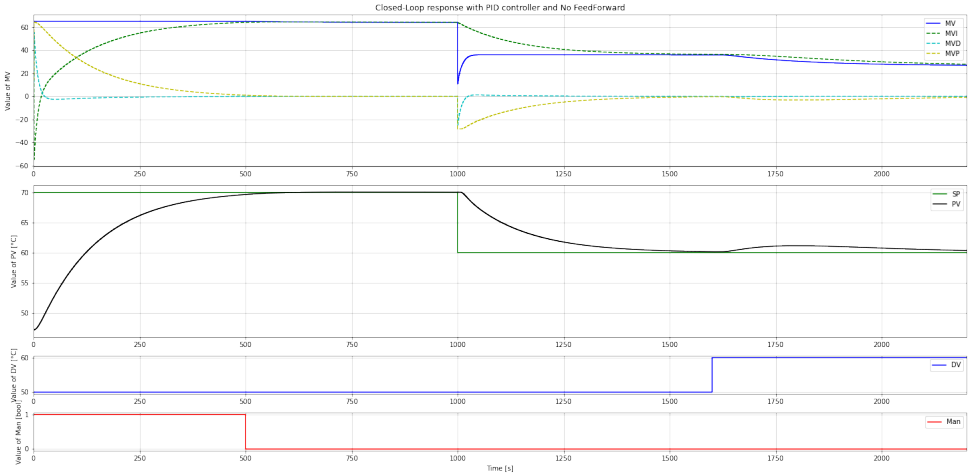

Figure 14: Closed-loop response without feedforward, highlighting the delayed compensatory action following the disturbance.

9.4 Closed-Loop Response with Feedforward (CLP FF)

The final scenario encompasses a closed-loop system enhanced with feedforward control, as shown in Figure 15. This setup demonstrates the most effective control strategy, where the PID controller addresses the error correction while the FF mechanism actively compensates for changes in DV. The system's response is swift and accurate, with the PV adhering closely to the SP, showcasing the synergy between closed-loop control and feedforward mechanisms.

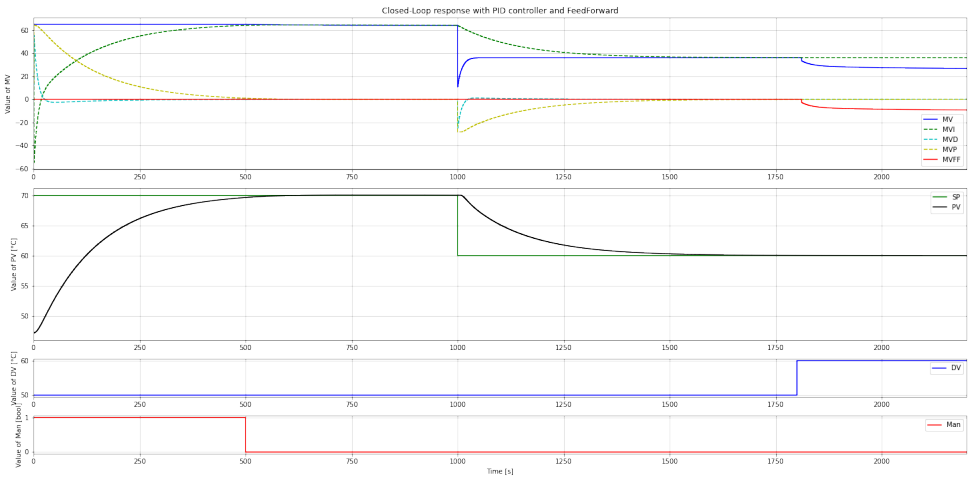

Figure 15: Closed-loop system response with feedforward, exhibiting rapid and precise PV adjustment to both SP and DV variations.

9.5 System Dynamics and Control Analysis

The simulations reveal several key dynamics of the control system:

- In an open-loop without FF, the system does not react to disturbances, which leads to a significant SP and PV gap.
- With FF in an open-loop, the system can counteract disturbances, but lacks the corrective action that a PID loop provides.
- In closed-loop control without FF, the system reacts to the error between SP and PV, yet the response to disturbances is delayed due to the lack of predictive adjustment.
- The inclusion of FF in a closed-loop significantly improves the system's resilience to disturbances, allowing for both corrective and anticipatory control actions.

Through the contrasting scenarios, it becomes apparent that combining PID control with feedforward mechanisms in a closed-loop system offers the best performance in terms of stability, responsiveness, and disturbance rejection.

10 Real-Time TCLab Experimentation

This section provides a comprehensive analysis of the TCLab kit's response to various control strategies implemented through PID and feedforward (FF) mechanisms. Four distinct experimental scenarios are considered: two each under open-loop (OLP) and closed-loop (CLP) configurations, with and without feedforward control.

10.1 Open-Loop Response without Feedforward (OLP No FF)

In the OLP No FF scenario, the system is subject to a disturbance increase at $t = 1300s$. The manual control (Man) is kept active throughout the experiment, indicating that the PID controller does not automatically adjust the manipulated variable (MV). Thus, the process variable (PV) reflects only the passive response to the disturbance variable (DV) with no compensatory control actions. The PV initially follows the setpoint (SP); however, upon the introduction of the disturbance, the PV deviates, illustrating the system's inability to counteract unanticipated changes without active control intervention.

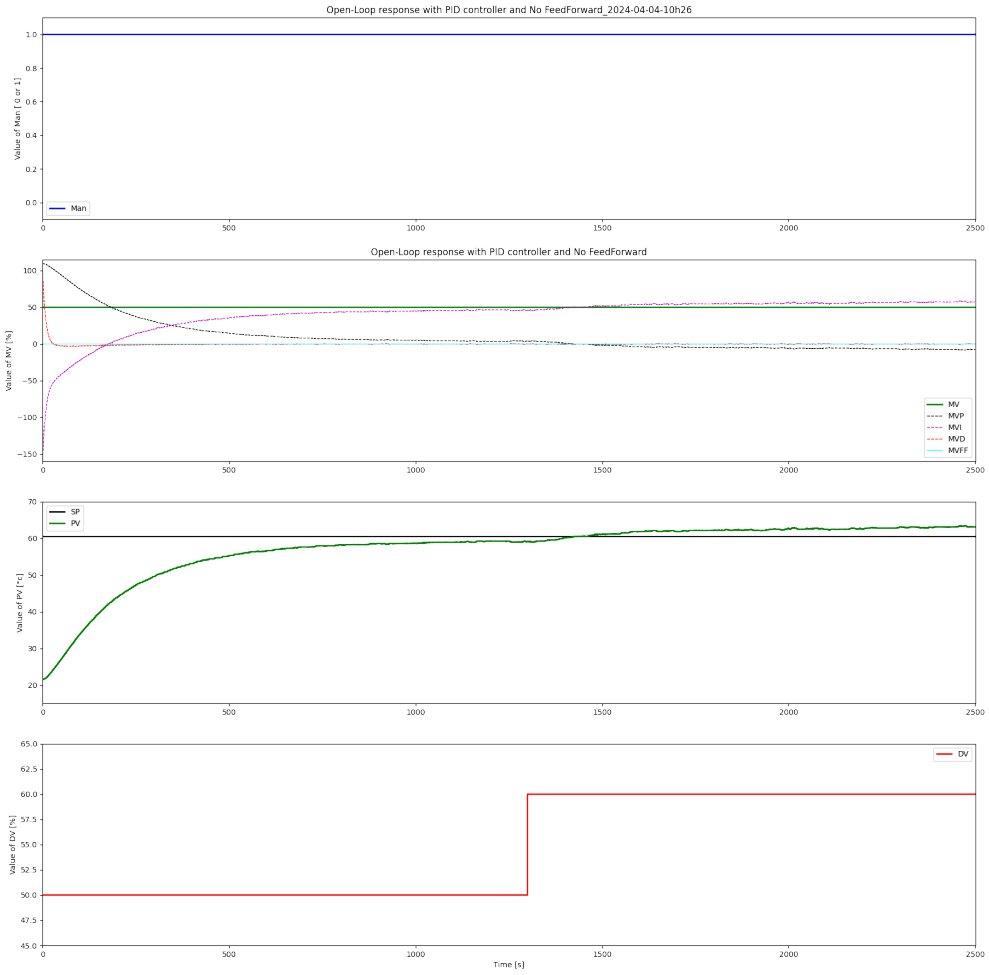

Figure 16: Open-loop response without feedforward control.

10.2 Open-Loop Response with Feedforward (OLP FF)

When feedforward is activated in the OLP FF scenario, the system anticipates the disturbance, and the MV is proactively adjusted to mitigate its impact. Although still in manual mode, the feedforward action allows the system to better maintain the PV at the desired SP despite the disturbance. The MV, influenced by the feedforward calculation, attempts to offset the expected effect of the disturbance, leading to a reduced deviation of PV from SP as compared to the OLP No FF scenario.

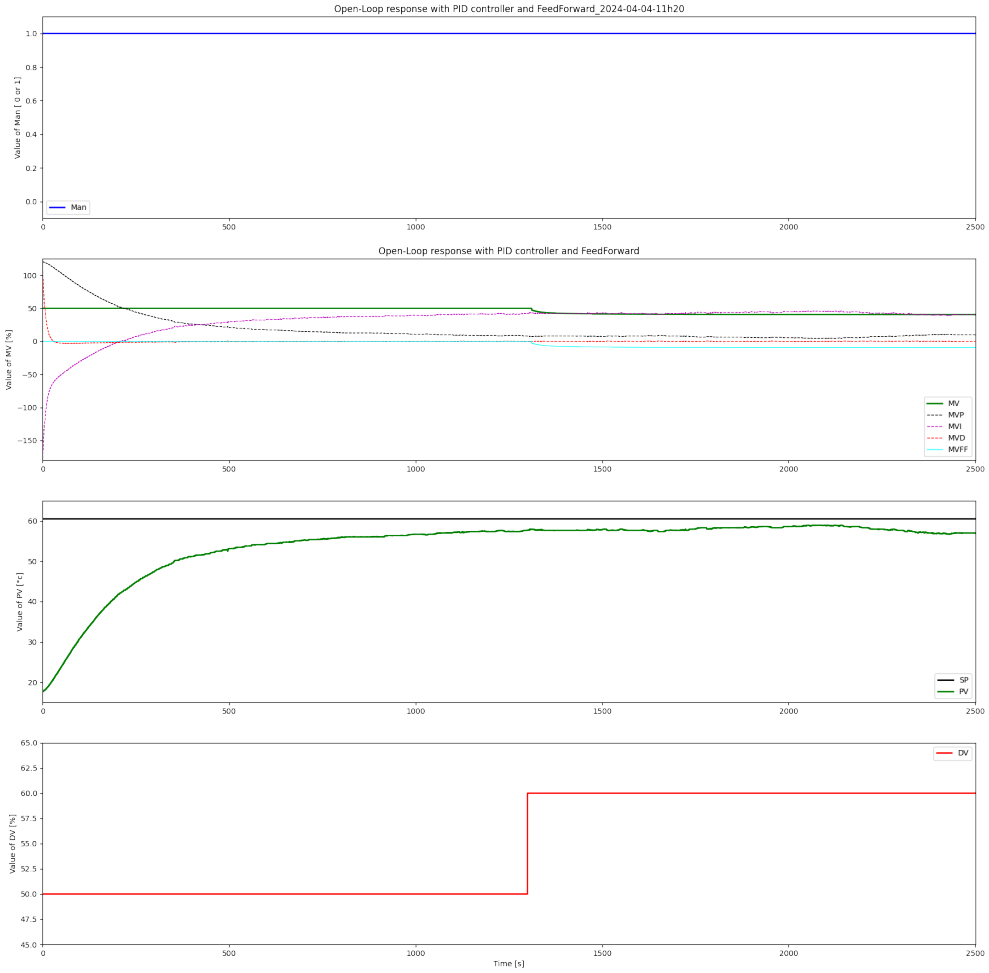

Figure 17: Open-loop response with feedforward control.

10.3 Closed-Loop Response without Feedforward (CLP No FF)

Transitioning to a closed-loop operation, the CLP No FF scenario employs a PID controller to automatically adjust MV in response to the error between SP and PV. The manual control is deactivated at $t = 500s$, transferring control to the PID. The SP changes at $t = 1200s$, and a disturbance is introduced at $t = 1700s$. The system's PV responds to the SP change and compensates for the disturbance. However, the response is not immediate due to the absence of feedforward, showcasing a reactive rather than proactive control strategy.

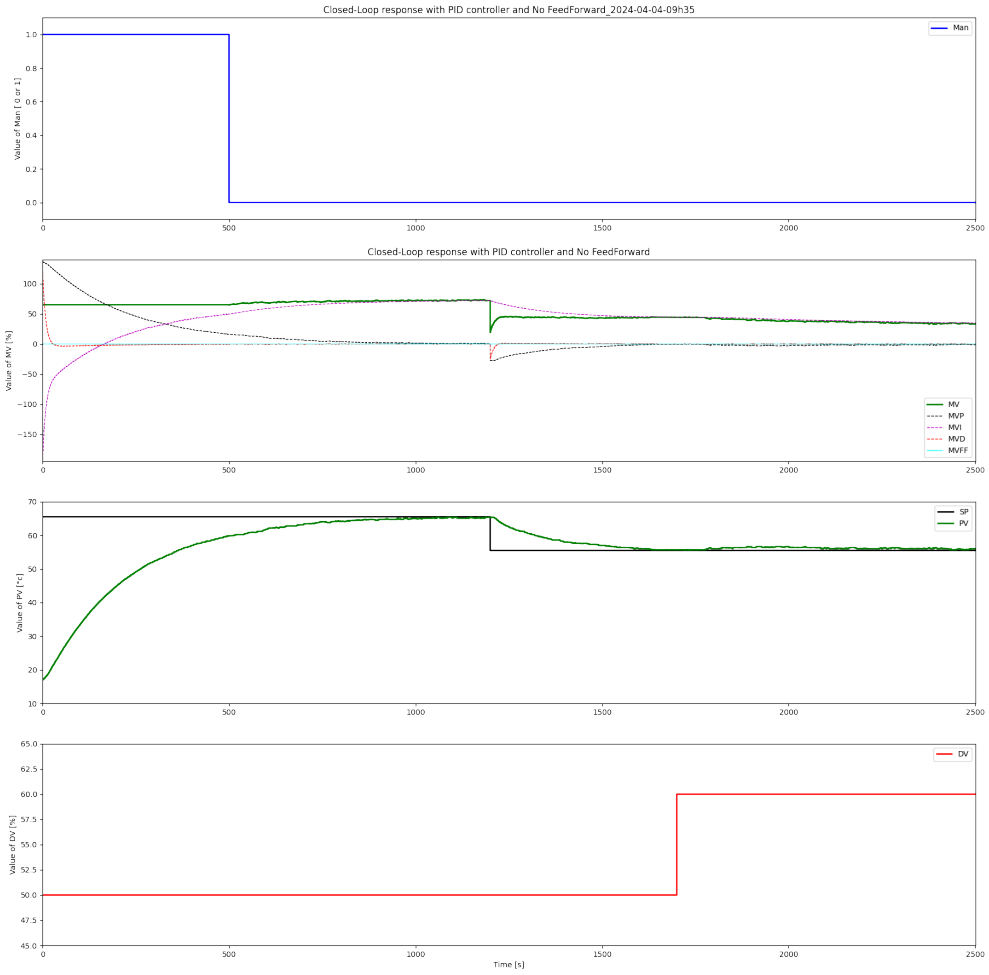

Figure 18: Closed-loop response without feedforward control.

10.4 Closed-Loop Response with Feedforward (CLP FF)

The CLP FF scenario demonstrates the most effective control strategy by combining the corrective action of the PID controller with the predictive nature of feedforward control. The feedforward anticipates the disturbance introduced at $t = 1900s$ and adjusts the MV accordingly. The result is a rapid and precise adjustment of the PV, maintaining it closely to the SP throughout the experiment. The synergy between the PID and FF control actions yields a robust control system that effectively rejects disturbances with minimal deviation from the SP.

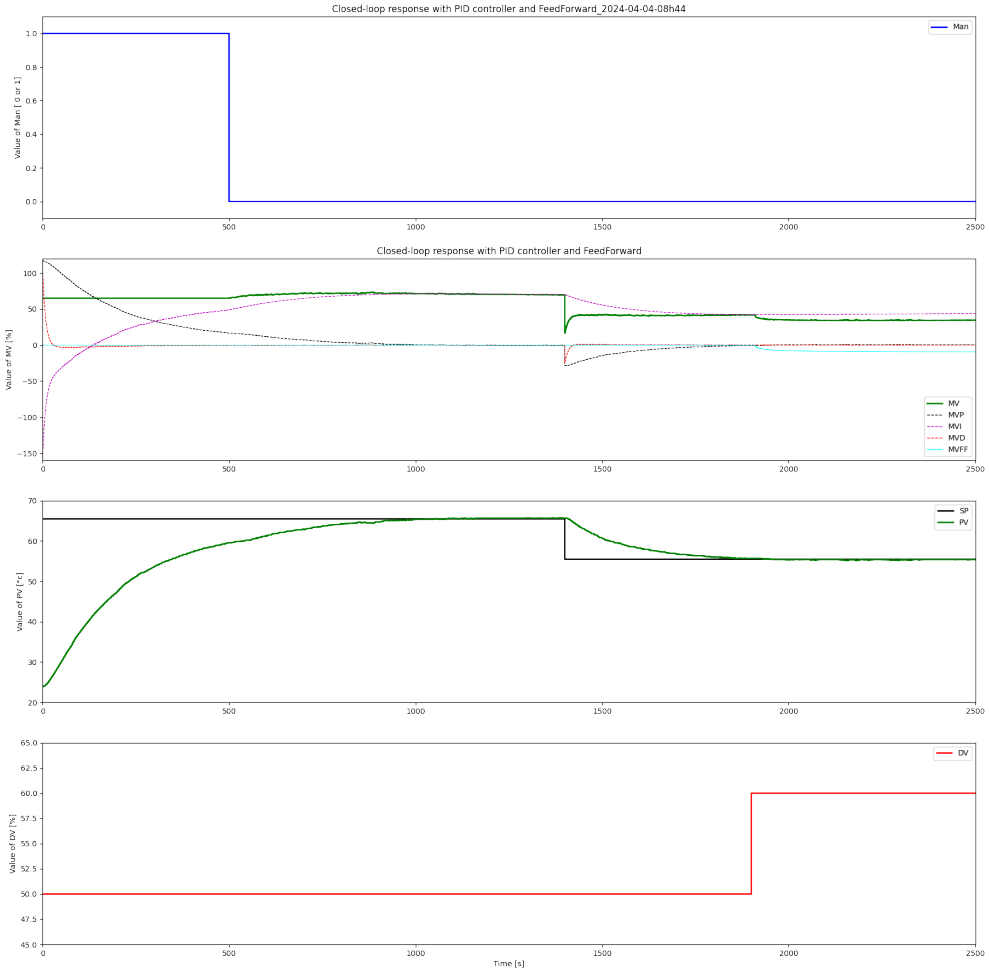

Figure 19: Closed-loop response with feedforward control.

10.5 Comparative Discussion

Real-time experimentation with the TCLab kit brings to light the importance of integrating various control strategies to handle disturbances and track setpoints effectively. The open-loop experiments highlight the impact of feedforward control in maintaining system performance in the face of external disturbances. The closed-loop experiments, particularly the scenario with both PID and feedforward control, illustrate the benefits of combining both corrective and anticipatory control actions for superior disturbance rejection and setpoint tracking. The real-time responses validate the simulation outcomes, reinforcing the advantages of a multifaceted control approach in practical applications.

11 Conclusion

This report has detailed the experimental validation and application of PID control with feedforward mechanisms using the TCLab kit. Through a structured approach encompassing open-loop tests, model identification, and closed-loop control, the practical intricacies of thermal system regulation were explored.

The laboratory exercises confirmed the theoretical principles of control theory and their effectiveness in real-world scenarios. The SOPDT models derived from experimental data provided a robust foundation for controller tuning. In particular, the use of feedforward control in conjunction with PID control showcased a significant improvement in system performance, demonstrating its utility in managing disturbances and maintaining the process variable at the setpoint.

Real-time experiments underscored the necessity of a comprehensive control strategy, especially in the presence of external perturbations. The findings from these experiments not only solidified the concepts learned but also highlighted the importance of integrating various control strategies to optimize system responsiveness and stability.

In conclusion, the experiments and analyses conducted have significantly contributed to a deeper understanding of control system design and implementation. They have reinforced the relevance of control theory in practical applications and opened avenues for continued learning and exploration in the field of control engineering.

12 Appendices

12.1 Mathematical Developments

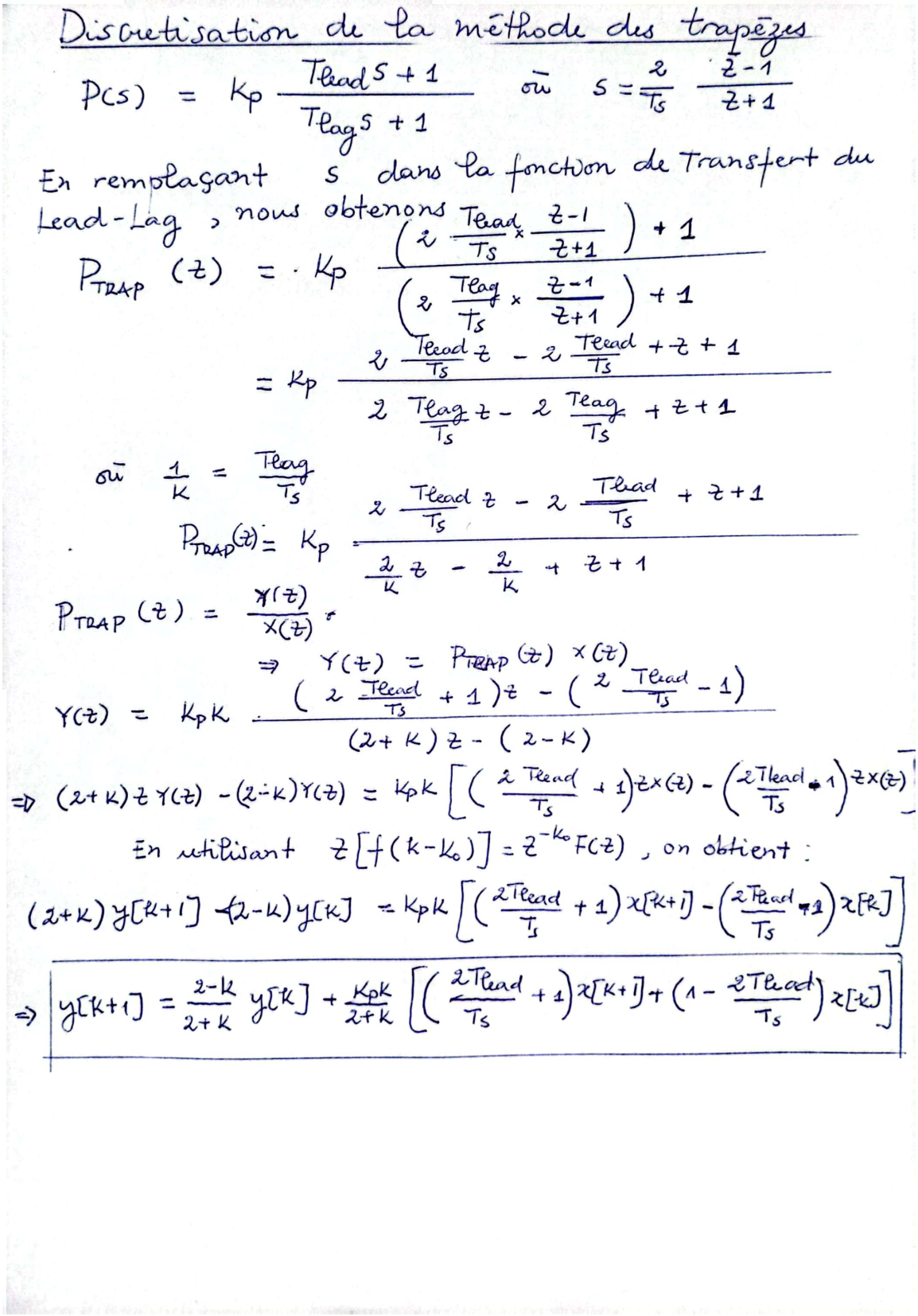

Discretisation de la méthode des trapèzes

$$P(s) = K_p \frac{T_{lead}s + 1}{T_{lag}s + 1} \quad \text{où} \quad s = \frac{2}{T_s}\frac{z-1}{z+1}$$

En remplaçant s dans la fonction de Transfert du Lead-Lag, nous obtenons

$$P_{TRAP}(z) = K_p \frac{\left(2\frac{T_{lead}}{T_s} \times \frac{z-1}{z+1}\right) + 1}{\left(2\frac{T_{lag}}{T_s} \times \frac{z-1}{z+1}\right) + 1}$$

$$= K_p \frac{2\frac{T_{lead}}{T_s}z - 2\frac{T_{lead}}{T_s} + z + 1}{2\frac{T_{lag}}{T_s}z - 2\frac{T_{lag}}{T_s} + z + 1}$$

où $\frac{1}{K} = \frac{T_{lag}}{T_s}$

$$P_{TRAP}(z) = K_p \frac{2\frac{T_{lead}}{T_s}z - 2\frac{T_{lead}}{T_s} + z + 1}{\frac{2}{K}z - \frac{2}{K} + z + 1}$$

$$P_{TRAP}(z) = \frac{Y(z)}{X(z)}$$

$$\Rightarrow Y(z) = P_{TRAP}(z) \times X(z)$$

$$Y(z) = K_p K \frac{\left(2\frac{T_{lead}}{T_s} + 1\right)z - \left(2\frac{T_{lead}}{T_s} - 1\right)}{(2+K)z - (2-K)}$$

$$\Rightarrow (2+K)zY(z) - (2-K)Y(z) = K_pK\left[\left(2\frac{T_{lead}}{T_s} + 1\right)zX(z) - \left(2\frac{T_{lead}}{T_s} - 1\right)zX(z)\right]$$

En utilisant $\mathcal{Z}[f(k-k_0)] = z^{-k_0}F(z)$, on obtient :

$$(2+K)y[k+1] - (2-K)y[k] = K_pK\left[\left(2\frac{T_{lead}}{T_s} + 1\right)x[k+1] - \left(2\frac{T_{lead}}{T_s} - 1\right)x[k]\right]$$

$$\Rightarrow \boxed{y[k+1] = \frac{2-K}{2+K}y[k] + \frac{K_pK}{2+K}\left[\left(2\frac{T_{lead}}{T_s} + 1\right)x[k+1] + \left(1 - 2\frac{T_{lead}}{T_s}\right)x[k]\right]}$$